

Electrical, Optical, Structural, and Analytical Properties of Very Pure GaN

D.C. Look

Semiconductor Research Center, Wright State University, Dayton, OH 45435

J.R. Sizelove

Air Force Research Laboratory, AFRL/MLPS, Wright-Patterson AFB, OH 45433

J. Jasinski and Z. Liliental-Weber

Lawrence Berkeley National Laboratory, 1 Cyclotron Road, Berkeley, CA 94720

K. Saarinen

Helsinki University of Technology, P.O. Box 1100, FIN-02015, Espoo, Finland

S.S. Park and J.H. Han

Samsung Advanced Institute of Technology, P.O. Box 111, Suwon, Korea, 440-600

ABSTRACT

Present hydride vapor phase epitaxial growth of GaN on Al_2O_3 can produce material of very high quality, especially in regions of the crystal far from the substrate/epilayer interface. In the present study, we characterize a 248- μm -thick epilayer, which had been separated from its Al_2O_3 substrate and etched on top and bottom to produce flat surfaces. Temperature-dependent Hall-effect data have been fitted to give the following parameters: mobility $\mu(300) = 1320 \text{ cm}^2/\text{V-s}$; $\mu(\text{peak}) = 12,000 \text{ cm}^2/\text{V-s}$; carrier concentration $n(300) = 6.27 \times 10^{15} \text{ cm}^{-3}$; donor concentration $N_D = 7.8 \times 10^{15} \text{ cm}^{-3}$; acceptor concentration $N_A = 1.3 \times 10^{15} \text{ cm}^{-3}$; and effective donor activation energy $E_D = 28.1 \text{ meV}$. These mobilities are the highest ever reported in GaN, and the acceptor concentration, the lowest. Positron annihilation measurements give a Ga vacancy concentration very close to N_A , showing that the dominant acceptors are likely native defects. Secondary ion mass spectroscopic measurements show that N_D is probably composed of the common donors O and Si, with $[\text{O}] > [\text{Si}]$. Transmission electron microscopy measurements yield threading dislocation densities of about $1 \times 10^7 \text{ cm}^{-2}$ on the bottom (N) face, and $< 5 \times 10^5 \text{ cm}^{-2}$ on the top (Ga) face. Photoluminescence (PL) spectra show a strong donor-bound exciton ($D^0\text{X}$) line at 3.47225 eV, and a weaker one at 3.47305 eV; each has a linewidth of about 0.4 meV. In the two-electron satellite region, a strong line appears at 3.44686 eV, and a weaker one at 3.44792 eV. If the two strong lines represent the same donor, then $E_{D,n=1} - E_{D,n=2} = 25.4 \text{ meV}$ for that donor, and the ground-state activation energy ($E_C - E_{D,n=1}$) is $(4/3)25.4 = 33.9 \text{ meV}$ in a hydrogenic

model, and 32.7 meV in a somewhat modified model. The measured Hall-effect donor energy, 28.1 meV, is smaller than the PL donor energy, as is nearly always found in semiconductors. We show that the difference in the Hall and PL donor energies can be explained by donor-band conduction via overlapping donor excited states, and the effects of non-overlapping excited states which should be included in the n vs. T data analysis (charge balance equation).

INTRODUCTION

Although GaN growth techniques have been developing over a period of more than thirty years[1], the high incorporation of impurities and defects still remains a major issue. Perhaps the dominant reason is that most of the growths are carried out on mismatched substrates, such as Al_2O_3 , leading to a high strain and a strong diffusion of both impurities and point defects from the substrate [2]. Threading dislocations are also extremely dense ($> 10^{10} \text{ cm}^{-2}$) near the substrate/epilayer interface, but diminish toward the surface because of annihilation processes [3]. Thus, the average quality of a typical layer is nearly always dependent upon thickness. Hydride vapor phase epitaxy (HVPE) has a high growth rate ($\sim 100 \mu\text{m}$ per hr), and thus is capable of growing thick material, up to $1000 \mu\text{m}$ in some cases [4-6]. For such a thick layer, a standard surface-sensitive characterization technique, such as photoluminescence (PL), will find a large difference in the quality of the top and bottom surface regions. Hall-effect measurements, on the other hand, will sample the whole crystal, and, in fact, will be strongly influenced by a thin, very conductive epilayer/substrate interface region, which always appears in HVPE GaN layers grown on Al_2O_3 [2,7]. Corrections for the interface region can be easily implemented if the sample can be modeled as two parallel layers, bulk and interface, and if the interface layer is totally degenerate [7]. Although this model has attained some success, and is widely used, still it is an approximation. Thus, for example, the donor activation energy E_D , obtained from a fit of the corrected temperature-dependent Hall-effect (T-Hall) data, may suffer from the inaccuracy of the two-layer model. In particular, a reliable comparison of the Hall and PL donor energies, long an issue in semiconductor circles, is made difficult.

Recently, such HVPE wafers have been proposed as a solution to the GaN substrate problem because, unlike the cases in Si, GaAs, SiC, and ZnO, large-area wafers of GaN cannot be obtained by bulk-growth techniques. However, since thick HVPE GaN layers can be grown on Al_2O_3 substrates, and since they can be easily separated from the Al_2O_3 substrates by a laser irradiation technique [5,6], they can possibly serve as GaN substrates for further GaN epitaxial growth. However, one problem with these separated wafers is a strong bow, due to the strain caused by the mismatched growth. This bow necessitates lapping, etching, and polishing both top and bottom surfaces in order to produce a flat wafer. In the Samsung procedure, the GaN layer is grown to a thickness of about 500 μm , and then about 100 μm of material are removed from each of the surfaces. From a characterization point of view, removal of 100 μm from the bottom surface eliminates the conductive interface layer, and a large portion of the dislocations and diffused impurities and point defects. Thus, the Hall-effect measurements on the final wafer are representative of the true, bulk material, and can be meaningfully compared with the PL results. Here, we examine the structural, analytical, optical, and electrical properties of a 248- μm Samsung wafer, S417, which exhibits the highest mobility ever reported in GaN. We also show that a rather simple model can reconcile the differences found between Hall and PL donor activation energies in this sample, and that this same model should be applicable to other samples and materials, also.

SECONDARY-ION MASS SPECTROSCOPY - IMPURITIES

Secondary-ion mass spectroscopy (SIMS) measurements [8] have been carried out on a GaN sample very similar to S417, but having a slightly inferior quality. These measurements give Si and O concentrations in the low-to-mid 10^{16} cm^{-3} , with $[\text{O}] > [\text{Si}]$. Another group has studied donors in Samsung material by far-IR absorption and SIMS techniques, and they have also concluded that O is the dominant donor [9]. Later, we will show that the total shallow, hydrogenic donor concentration N_D in S417 is $7.8 \times 10^{15} \text{ cm}^{-3}$, a somewhat lower value than $[\text{O}] + [\text{Si}]$, as determined by SIMS. However, SIMS measurements are not always accurate at these low concentrations, and, also, some of the O and Si may not be electrically active.

POSITRON ANNIHILATION SPECTROSCOPY - VACANCIES

Positrons injected into defect-free GaN are annihilated by electrons in a mean time of 160 – 165 ps. However, if there are negatively charged vacancies present, some of the positrons will become trapped at those locations, and will have longer lifetimes, because of the reduced electron density at vacancies. In the case of GaN, Ga vacancies (but not N vacancies) would be expected to fill this role, and indeed, PAS has been used to identify and quantify V_{Ga} -related defects [10]. In fact, comparisons of V_{Ga} concentrations with acceptor concentrations N_{A} in a series of undoped, n-type HVPE GaN samples, with N_{A} ranging from 10^{15} to 10^{19} cm^{-3} , show that $[V_{\text{Ga}}] \approx N_{\text{A}}$, to within experimental error [2,10]. In particular, a Samsung HVPE GaN sample with properties very similar to those of S417 has been shown to have $[V_{\text{Ga}}] \approx 2 \times 10^{15} \text{ cm}^{-3}$ [11], very close to our value of N_{A} determined by Hall-effect measurements, discussed below. Thus, it appears that V_{Ga} , and not any impurity, is the dominant acceptor in HVPE GaN, and probably in other types of undoped GaN, also. Indeed, theory predicts that V_{Ga} centers should be abundant in n-type GaN[12].

TRANSMISSION ELECTRON MICROSCOPY - DISLOCATIONS

Convergent beam electron diffraction analysis shows that the bottom surface (closest to the Al_2O_3) is the N face, and the top surface, the Ga face. This, in fact, turns out to be the case for most HVPE-grown GaN/ Al_2O_3 layers. Transmission electron microscopy results for the Ga face, shown in Fig. 1, show very few threading dislocations, with $N_{\text{dis}} < 5 \times 10^5 \text{ cm}^{-2}$. This is one of the lowest results ever reported in heteroepitaxial GaN, and suggests that such wafers could be used for many commercial purposes. On the N face, the number is somewhat higher: $N_{\text{dis}} \leq 1 \times 10^7 \text{ cm}^{-2}$, but it is likely that the Ga face would be used for most subsequent epitaxial growth.

PHOTOLUMINESCENCE - DONORS

A 4-K PL spectrum of the near-band-edge (exciton) region, 3.465 – 3.480 eV, is shown in Fig. 2. The sharp lines at 3.47123, 3.47225, and 3.47305 eV are likely neutral donor-bound A excitons (D^0X_{AS}), while the broader line at 3.47921 eV is the free A exciton X_A . The line at 3.47609 eV may be an excited (rotator) state of a D^0X_A , or possibly a D^0X_B transition. It has been reported that the D^0X_A line in unstrained material should lie at 3.471 - 3.472 eV, a result that suggests immediately that the present Samsung wafer does not have a high strain. This is expected, since strain decreases with thickness. The full width at half maximum (FWHM) for each of the D^0X lines is about 0.4 meV, which indicates excellent material; however, for *homoepitaxial* layers, even better FWHM values, 0.1 meV, have been reported [13]. Another group of PL lines appears in the region 3.440 – 3.455 eV, with a strong line at 3.44686 eV and a weaker one at 3.44792 eV. This region should include two-electron satellite (TES) replicas of the D^0X transitions. That is, if the collapse of an exciton bound to a neutral donor leaves the donor in an $n=2$ state, rather than the usual $n=1$ state, then the difference in energy should be $E_{D,n=2} - E_{D,n=1} = 3R/4$, where R is the Rydberg for GaN ($R = 13.6m^*/\epsilon_0^2$ eV). By shifting the entire spectrum up by 25.4 meV, in order to overlay the strongest D^0X line onto the strongest TES line, we see in Fig. 3 that these two lines have very similar shapes and thus probably correspond to the same donor. If so, the GaN Rydberg should be about $4(25.4)/3 = 33.9$ meV. However, this calculation presumes that the donor is fully hydrogenic, which is often not true in semiconductors, especially for the ground state ($n=1$). For a more accurate determination of R , Moore et al. [9] have compared 2p and 3p states, seen in absorption, because these states should be nearly hydrogenic, i.e., they should have small central-cell corrections. From the fact that the energy difference between the 2p and 3p states in the hydrogenic model is $(1/4 - 1/9)R$, Moore et al. have determined that $R = 29.1$ meV. If this value of R is correct, then the true ground state of our main donor is $E_{D,n=1} - E_{D,n=2} + R/4 = 32.7$ meV, i.e., 3.6 meV above the Rydberg. This means that there must be an additional attractive force acting in conjunction with the donor core. However, we must reserve judgment on this issue, because the positions of some weaker (3s and 4s) TES lines, compared with that of the strongest (2s) TES line, is more consistent with an energy of 33.9 meV, rather than 32.7 meV. Below, we will compare the PL-derived donor energy with that determined by Hall-effect analysis.

HALL-EFFECT MEASUREMENTS – DONORS AND ACCEPTORS

The basic equations for Hall-effect analysis, allowing for the energy \mathcal{E} dependence of the electrons, are as follows [14]:

$$j_x = \frac{ne^2 \langle \tau \rangle}{m^*} E_x \equiv -ne\mu_c E_x \quad (1)$$

$$R_H = \frac{E_y}{j_x B} = -\frac{1}{ne} \frac{\langle \tau^2 \rangle}{\langle \tau \rangle^2} = -\frac{r}{ne} \quad (2)$$

where j_x is the current density, E_x and E_y are the electric field vectors, $B_z = B$, the magnetic field strength, τ the relaxation time, R_H , the Hall coefficient, and

$$\langle \tau^n(E) \rangle = \frac{\int_0^\infty \tau^n(E) E^{3/2} \frac{\partial f_0}{\partial E} dE}{\int_0^\infty E^{3/2} \frac{\partial f_0}{\partial E} dE} \rightarrow \frac{\int_0^\infty \tau^n(E) E^{3/2} e^{-E/kT} dE}{\int_0^\infty E^{3/2} e^{-E/kT} dE} \quad (3)$$

This formulation is called the relaxation-time approximation to the Boltzmann Transport Equation. Here f_0 is the Fermi-Dirac distribution function and the second equality in Eq. 3 holds for non-degenerate electrons, i.e., those describable by Boltzmann statistics. The quantity $\mu_c = e\langle \tau \rangle/m^*$ is known as the “conductivity” mobility, since the quantity $ne\mu_c$ is just the conductivity σ . We define the “Hall” mobility as $\mu_H = R_H \sigma = r\mu_c$, and the “Hall” concentration as $n_H = n/r = -1/eR_H$. Thus, a combined Hall-effect and conductivity measurement gives n_H and μ_H , although we would prefer to know n , not n_H ; fortunately, however, r is usually within 20% of unity, and is almost never as large as two. In any case, r can often be calculated or measured so that an accurate value of n can usually be determined.

The relaxation time, $\tau(\mathcal{E})$, depends upon how the electrons interact with the lattice vibrations as well as with extrinsic elements, such as charged impurities and defects. For example, acoustical-mode lattice vibrations scatter electrons through the deformation potential (τ_{ac}) and piezoelectric potential (τ_{pe}); optical-mode vibrations through the polar potential (τ_{po}); ionized impurities and defects through the screened coulomb potential (τ_{ii}); and charged dislocations, also through the coulomb potential (τ_{dis}). The strengths of these various scattering mechanisms depend upon certain lattice parameters, such as

dielectric constants and deformation potentials, and extrinsic factors, such as donor, acceptor, and dislocation concentrations, N_D , N_A , and N_{dis} , respectively [14-16]. The total momentum scattering rate, or inverse relaxation time, is

$$\tau^{-1}(\mathcal{E}) = \tau_{ac}^{-1}(\mathcal{E}) + \tau_{pe}^{-1}(\mathcal{E}) + \tau_{po}^{-1}(\mathcal{E}) + \tau_{ii}^{-1}(\mathcal{E}) + \tau_{dis}^{-1}(\mathcal{E}) \quad (4)$$

and this expression is then used to determine $\langle \tau^n(\mathcal{E}) \rangle$ via Eq. 3, and thence, $\mu_H = e\langle \tau^2 \rangle / m^* \langle \tau \rangle$. Formulas for τ_{ac} , τ_{pe} , τ_{po} , τ_{ii} , and τ_{dis} , can be found in the literature, and, fortunately, the only unknowns in Eq. 1-4, are N_D , N_A , and N_{dis} . For our sample, N_{dis} is very small, and furthermore, N_D can be written in terms of n and N_A . Thus, the only unknown in the μ_H vs. T fit is N_A .

The fitting of μ_H vs. T data should be carried out in conjunction with the fitting of n vs. T data, and the relevant expression here is the charge-balance equation (CBE) [14]:

$$n + N_A = \frac{N_D}{1 + n / \phi_D} \quad (5)$$

where we have assumed only one type of donor, with a single charge state, and where

$$\phi_D = \frac{g_0}{g_1} e^{\frac{\alpha_D}{k}} N_C' T^{3/2} e^{-\frac{E_{D0}}{kT}} \quad (6)$$

Here, g_0/g_1 is a degeneracy factor, $N_C' = 2(2\pi m_n^* k)^{3/2} / h^3$ is the effective conduction-band density of states at 1K, h is Planck's constant, E_D is the donor ground-state energy, and E_{D0} and α_D are defined by $E_D = E_{D0} - \alpha_D T$. If more than one donor is needed to fit the data, then equivalent terms are added on the right hand side of Eq. 5. Examples of common, single-charge-state donors in GaN are Si on a Ga site, and O on an N site. If there are double or triple donors, or more than one acceptor, proper variations of Eq. 5 can be found in the literature [14].

If the donors are effective-mass-like, they will have a set of excited states, much like those of hydrogen. Using standard statistical analysis, we can add hydrogenic-type excited states ($j = 2, 3, \dots, m$) to the analysis by modifying ϕ_D [14,17].

$$\phi_D = \frac{g_0}{g_1} e^{\frac{\alpha_D}{k}} N_C T^{3/2} \frac{e^{-\frac{E_{D0}}{kT}}}{1 + \sum_2^m j^2 e^{-\left(1 - \frac{1}{j^2}\right) \frac{E_{D0}}{kT}}} \quad (7)$$

where we have assumed that $g_j/g_0 = j^2$, as is the case for the hydrogen atom, and also that α_D is the same for each state. (Actually, in any case, α_D should be small for an effective-mass-like donor state.) At low temperatures, only the ground state will be occupied, and the additional term in the denominator of Eq. 7 will be small. However, at higher temperatures, the n vs. T curve will be modified. To see the effects of excited states in GaN, we plot $\ln(n)$ vs. $1/T$ for the case of 0, 2, and 10 excited states. Here, we have assumed parameters appropriate for the present sample: $E_{D0} = 32.7$ meV (O_N), $g_0 = 1$, $g_1 = 2$, $\alpha_D = 0$, $m^* = 0.22 m_0$, $N_D = 7.8 \times 10^{15} \text{ cm}^{-3}$, and $N_A = 1.3 \times 10^{15} \text{ cm}^{-3}$. As seen in Fig. 4, two excited states have only a small effect on the curve, but ten have a very large effect. However, is it reasonable to include ten or more excited states in the analysis? The answer is no, as argued below.

In the hydrogenic model, the orbital radius of the m^{th} excited state is $r_m = m^2 a_0$, where a_0 is the Bohr radius, $a_0 = 0.529 \epsilon_0 / m^*$. For GaN, m^* is well determined at $0.22 m_0$, and we can then get $\epsilon_0 = 10.14$ from Moore's determination [9] of the Rydberg, $R = 0.0291 \text{ eV} = 13.6 m^* / \epsilon_0^2$. So, $a_0 \approx 24 \text{ \AA}$ for GaN. For a given donor density N_D , the m^{th} orbitals will begin to overlap at the approximate condition $(4/3)\pi r_m^3 N_D = 1$. The energy of the m^{th} excited state, with respect to the conduction band, is $E_C - R/m^2 = E_C - R a_0 / r_m = E_C - [(1.16 \times 10^{-4})/\epsilon_0] N_D^{1/3} \text{ meV}$. For $\epsilon_0 = 10.14$, in GaN, this expression becomes $E_C - (1.14 \times 10^{-5}) N_D^{1/3} \text{ meV}$. Because of the wavefunction overlap in the m^{th} orbital, donor-band conduction will begin to take place, so that the *effective* conduction-band minimum is lowered by R/m^2 , at least from a conductivity point of view. Or, equivalently, the effective donor energy is reduced by R/m^2 , or approximately E_{D0}/m^2 . We can now also see that it doesn't make sense to include excited states higher than m , because they are essentially in the conduction continuum [18]. For our sample, $N_D = 7.8 \times 10^{15} \text{ cm}^{-3}$, so that $r_m \approx 313 \text{ \AA}$, and thus $m = (r_m/a_0)^{1/2} \approx 3.58$. Allowing m to remain a non-integer, we

can then calculate the *predicted* Hall-effect donor energy in our example to be $32.7 - 29.1/12.83 = 30.4$ meV.

The Hall mobility μ_H data, and the theoretical fit are plotted vs. temperature in Fig. 5. From these data, an acceptor concentration $N_A = 1.3 \times 10^{15} \text{ cm}^{-3}$ is deduced, the lowest ever determined in GaN. The carrier concentration data, corrected for the Hall r -factor, are plotted in Fig. 6, along with the theoretical fit (Eq. 5). Here two donors are found from the fit: $N_{D1} = 7.8 \times 10^{15} \text{ cm}^{-3}$, $E_{D1} = 28.1$ meV; and $N_{D2} = 1.1 \times 10^{15} \text{ cm}^{-3}$, $E_{D1} = 53.2$ meV. Also, the fitted acceptor concentration N_A is $7.2 \times 10^{14} \text{ cm}^{-3}$, a little smaller than the value found from the mobility fit, but not considered to be as accurate as the latter. The main point here is that $E_D(\text{Hall}) < E_D(\text{PL})$ by a few meV, as predicted from the above analysis. Although the analysis predicts a difference of 2.3 meV, and the actual difference is 4.6 meV, still the crudeness of the wavefunction-overlap model would not be expected to give precise results. For example, the random nature of the donor distribution should be included. Also, there is one more factor to consider, i.e., the effects of *non-overlapping* excited states ($m = 2$ and 3, in this case).

At low temperatures, Eq. 5 can be written, $n = (N_D/N_A - 1)\phi_D$, and the donor activation energy is often determined by plotting $\ln(n/T^{3/2})$ vs. $1/T$. Including excited states in ϕ_D (Eq. 7), and ignoring the small difference between E_D and R , we can show that the slope of this plot is

$$\frac{d[\ln(n/T^{3/2})]}{d(1/T)} = -\frac{E_D}{k} \left\{ \frac{1 + \sum_2^m e^{-E_D(1-1/j^2)/kT}}{1 + \sum_2^m j^2 e^{-E_D(1-1/j^2)/kT}} \right\} \quad (8)$$

Clearly, the magnitude of the slope will be less than the typically assumed value, E_D/k ; however, the question is, how much less? In the present case, with wavefunction overlap predicted at $m = 3.58$, we should include only the $m = 2$ and 3 excited states in the analysis. Still, the value of the bracketed term in Eq. 8 cannot be calculated precisely, because it depends upon temperature. For $E_D = 30$ meV, the bracketed term is about 0.987 at $T = 40$ K, 0.969 at 50 K, and 0.923 at 60 K. For our sample, the low-temperature slope would best be determined at $T = 40$ K, and the existence of excited states would lower the measured slope here by about 1.3% of 29.1 meV, or about 0.4 meV. However,

fitting algorithms generally fit the whole curve, not just the low-temperature part; thus, it is difficult to predict the final fitted value of E_D , except that it will be too low if excited states are not properly included in the analysis.

CONCLUSIONS

The analysis of thick GaN layers grown by HVPE demonstrates that donor and acceptor concentrations below 10^{16} cm^{-3} , and 300-K mobilities above $1200 \text{ cm}^2/\text{V-s}$, can be reproducibly achieved [19]. The high purity is most likely due to the lower dislocation density in thick material, because dislocations can promote the diffusion of point defects and impurities from the substrate. Such high-quality material allows us to gain insight into the difference between the donor energies as measured by Hall-effect and photoluminescence measurements, a difference which is nearly universal in semiconductor research. By consideration of the two-electron satellite transitions seen in the PL measurements, and the value of the Rydberg in GaN, determined by another group [9], we find that the dominant donor (probably O_N , but possibly Si) has a ground-state energy of between 32.7 and 33.9 meV. The *measured* Hall-effect energy $E_D(\text{Hall})$, on the other hand, is expected to be less than the *true* ground-state energy, because: (1) donor-band conduction, which can occur as the excited-state orbitals begin to overlap, reduces the activation energy necessary for strong, band-type conductivity; and (2) non-overlapping excited states are typically (and wrongly) excluded when fitting n vs. T with the charge-balance equation (CBE). We calculate that the overlap effect should reduce $E_D(\text{Hall})$ by about 2.3 meV, for $N_D = 7.8 \times 10^{15} \text{ cm}^{-3}$, and that the failure to include excited states in the CBE analysis should further reduce $E_D(\text{Hall})$ by at least 0.4 meV, and perhaps more. (Note that care must be taken to include in the CBE only *non-overlapping* excited states, $m = 2$ and 3 in this case.) A conclusion of this investigation is that a true ground-state energy can, in principle, be found from PL data, but not from Hall data, unless N_D is very low and excited states are properly included in the analysis. However, the PL determination requires the observation of one or more TES lines, and also a good value for the GaN Rydberg, presently thought to be about 29.1 meV, but possibly higher.

There are also other explanations of why $E_D(\text{Hall}) < E_D(\text{PL})$. Perhaps the most common of these is that PL will mainly sample the lowest- N_D (highest E_D) parts of the sample, because those parts give the sharpest, most intense spectral lines, whereas Hall-effect measurements will sample the highest- N_D (lowest E_D) parts, because those parts conduct the most current. While this mechanism may be valid for samples with high inhomogeneity, the model we have proposed is valid in all cases, and indeed, is fundamental. An interesting corollary of our analysis is that when N_D is high enough that the $m=2$ orbitals began to overlap, then the PL TES lines (which usually derive from the $m=2$ orbitals) may be affected, and it may no longer be possible to get an accurate ground-state energy from PL data. From our analysis, this condition should occur at $N_D = 2.6 \times 10^{17} \text{ cm}^{-3}$ in GaN. Further research on these ideas should be conducted, especially on samples with different values of N_D .

ACKNOWLEDGMENTS

We wish to thank T.A. Cooper for the Hall-effect measurements, W. Rice for the PL measurements, W. Swider for TEM sample preparation, and the NCEM in Berkeley for the use of the TEM facility. We also would like to thank W.J. Moore for helpful discussions. DCL was supported under AFOSR Grant F49620-00-1-0347 and ONR Grant N00014-02-1-0606, and most of his work was carried out at the Air Force Research Laboratory, Wright-Patterson AFB, Ohio. JJ and ZL-W were supported by AFOSR, Order No. FQ86710200652, through the U.S. Department of Energy under Contract No. DE-AC03-76F00098.

REFERENCES

1. H.P. Maruska and J.J. Tietjen, Appl. Phys. Lett. **15**, 327 (1969).
2. D.C. Look, C.E. Stutz, R.J. Molnar, K. Saarinen, and Z. Liliental-Weber, Solid State Commun. **117**, 571 (2001).
3. J. Jasinski and Z. Liliental-Weber, J. Electron. Mater. **31**, 429 (2002).
4. R.J. Molnar, K.B. Nichols, P. Makai, E.R. Brown, and I. Melngailis, Mater. Res. Soc. Symp. Proc. **378**, 479 (1995).
5. S.S. Park, I-W. Park, and S.H. Choh, Jpn. J. Appl. Phys., Part 2 **39**, L1141 (2000).
6. E. Oh, S.K. Lee, S.S. Park, K.Y. Lee, I.J. Song, and J.Y. Han, Appl. Phys. Lett. **78**, 273 (2001).
7. D.C. Look and R.J. Molnar. Appl. Phys. Lett. **70**, 3377 (1997).
8. Evans East, 104 Windsor Center, East Windsor, NJ, 08520
9. W.J. Moore, J.A. Freitas, Jr., S.K. Lee, S.S. Park, and J.Y. Han, Phys. Rev. B **65**, 081201 (2002).
10. K. Saarinen, J. Nissilä, P. Hautojärvi, J. Likonen, T. Suski, I. Grzegory, B. Lucznik, and S. Porowski, Appl. Phys. Lett. **75**, 2441 (1999).
11. J. Oila, J. Kivioja, V. Ranki, K. Saarinen, D.C. Look, R.J. Molnar, and S.S. Park (to be published).
12. J. Neugebauer and C.G. Van de Walle, Phys. Rev. B **50**, 8067 (1994).
13. K. Kornitzer, T. Ebner, K. Thonke, R. Sauer, C. Kirchner, V. Schwegler, M. Kamp, M. Leszczynski, I. Grzegory, and S. Porowski, Phys. Rev. B **60**, 1471 (1999).
14. D.C. Look, *Electrical Characterization of GaAs Materials and Devices* (Wiley, New York, 1989), Ch.1.
15. D.L. Rode, Semicond. Semimetals **10**,1 (1975).
16. B.R. Nag, *Electron Transport in Compound Semiconductors* (Springer, Berlin, 1980).
17. D.V. Eddolls, J.R. Knight, and B.L.H. Wilson, in *Proc. Int. Symp. on GaAs*, ed. by J. Franks and W.G. Moore (Inst. Phys., London, 1967) pp.3-9.
18. G.E. Stillman and C.M. Wolfe, Thin Solid Films **31**, 69 (1976).
19. D.C. Look and J.R. Sizelove, Appl. Phys. Lett. **79**, 1133 (2001).

Fig. 1. Cross-sectional TEM micrograph of the region near the Ga face. Note the lack of dislocation features.

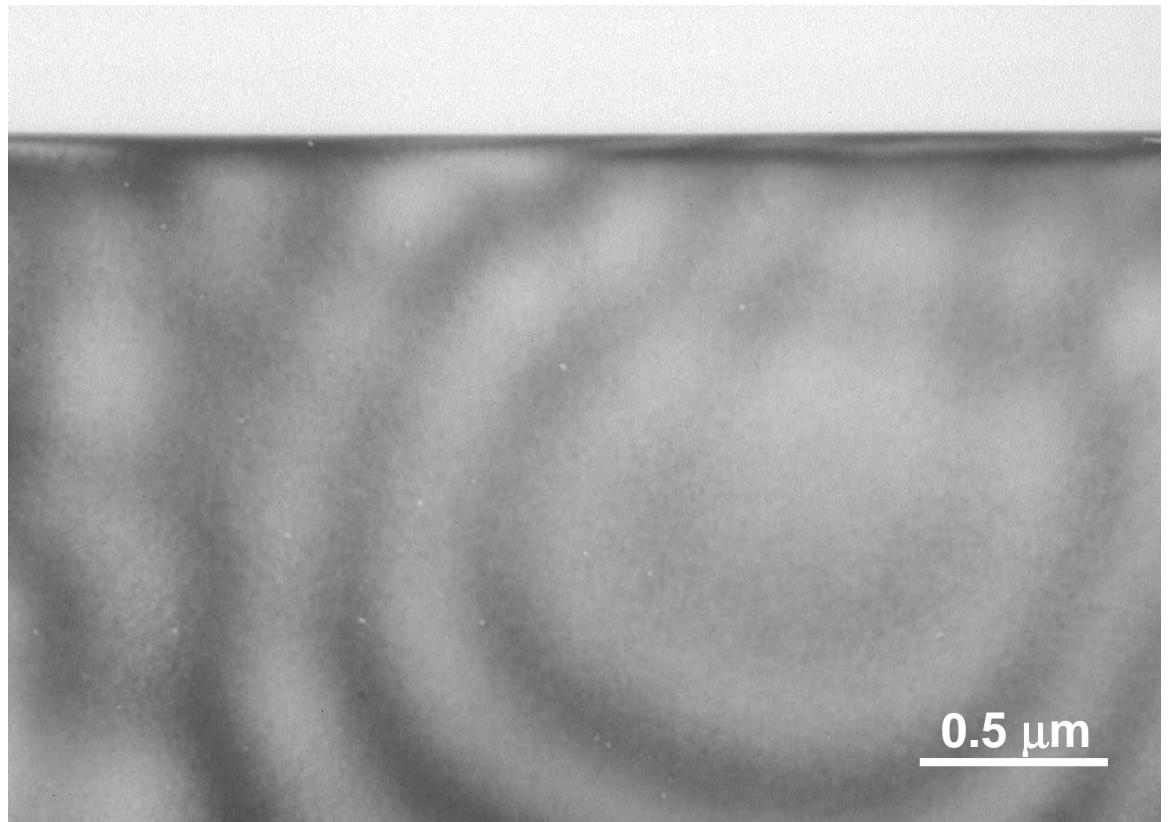


Fig. 2. Photoluminescence spectrum in exciton region. The portion of the spectrum above 3.475 eV has been multiplied by a factor 10, to emphasize the weak lines.

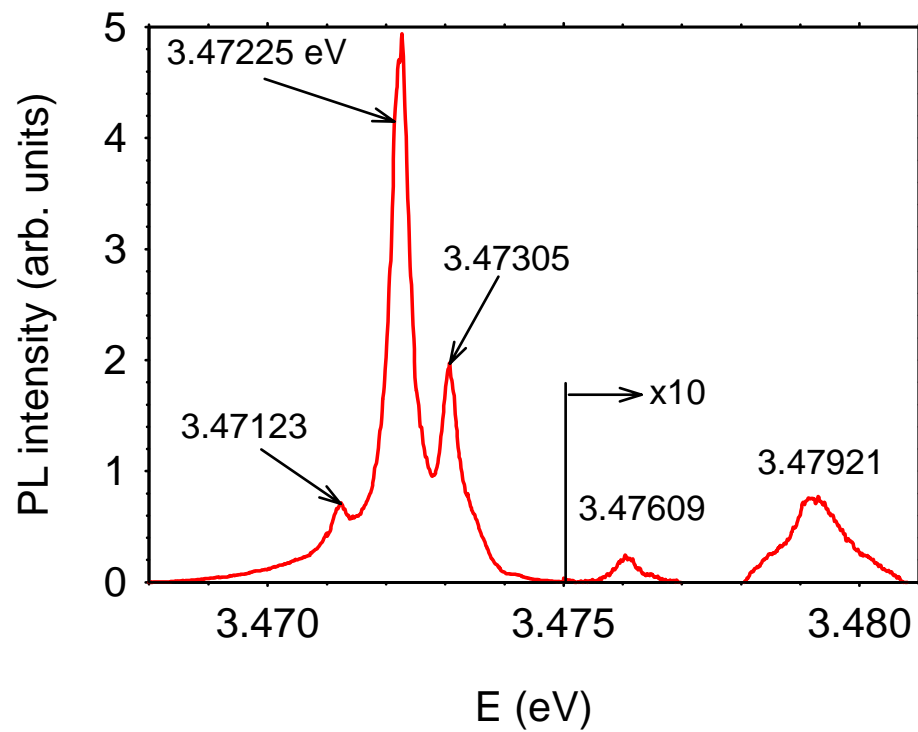


Fig. 3. Comparison of exciton lines (solid curve – unshifted), and TES lines (dashed curve – shifted up by 25.4 meV). The dashed curve has been multiplied by a factor 89 over the full range, while a portion of the solid curve, from 3.475 – 3.481 eV, has been multiplied by a factor 10.

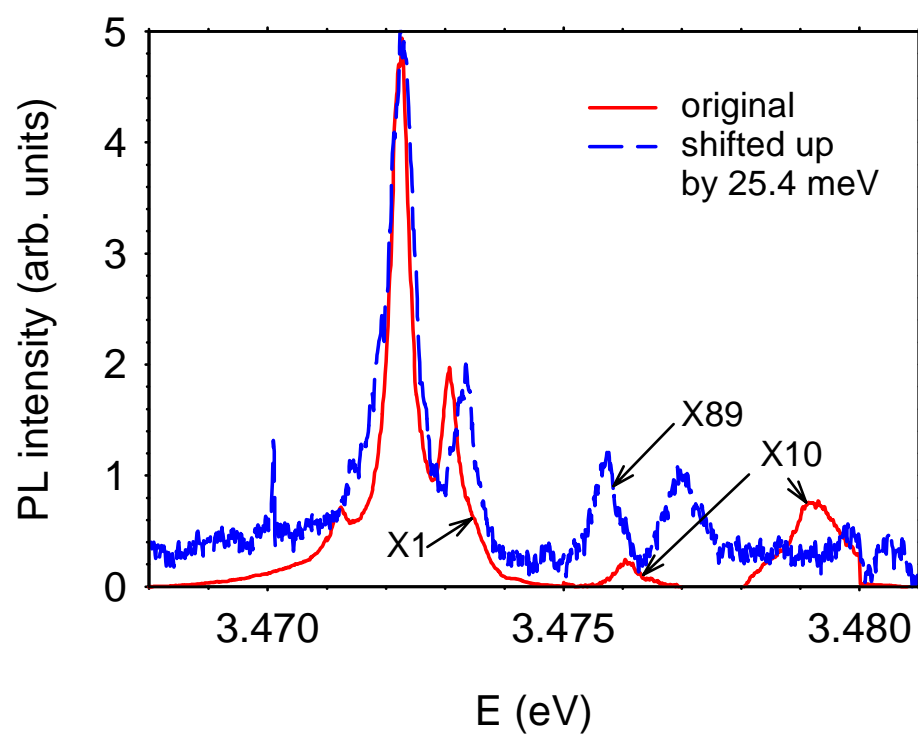


Fig. 4. Effects of donor excited states on simulated Hall-effect data.

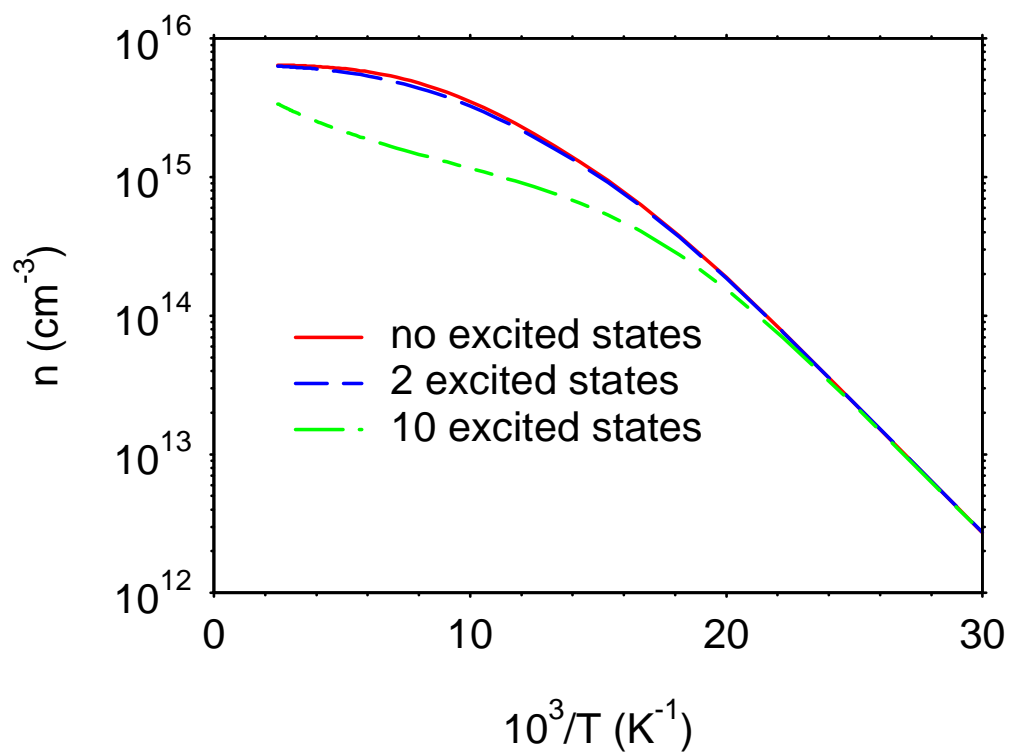


Fig. 5. Experimental and theoretical Hall mobility plots.

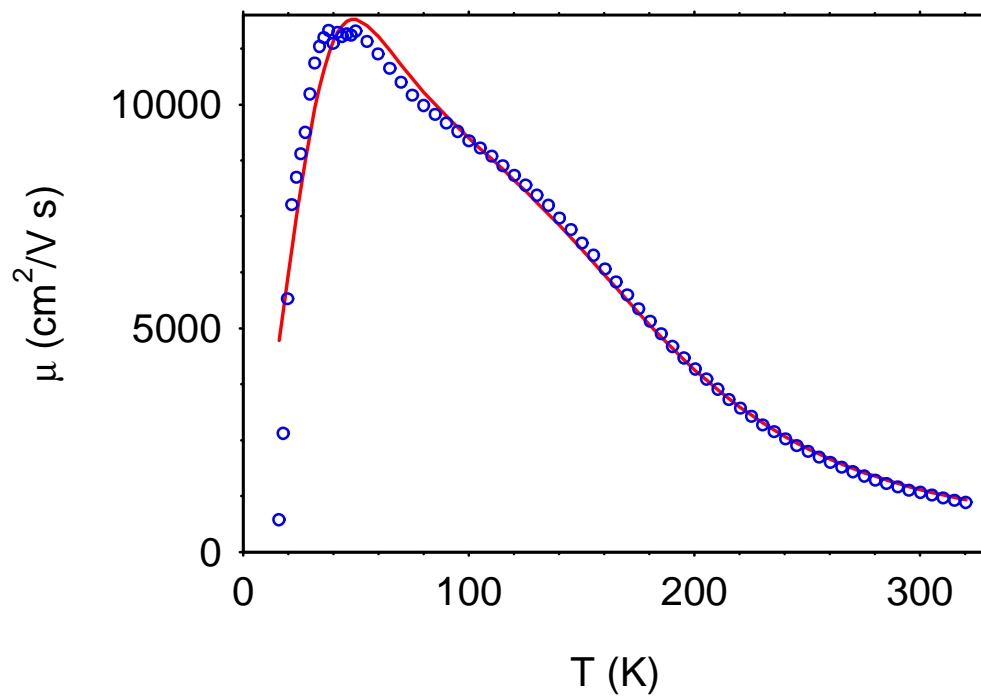


Fig 6. Experimental and theoretical carrier concentration plots.

